arXiv:cond-mat/0306399v1 [cond-mat.supr-con] 16 Jun 2003

Vorticity, phase stiffness and the cuprate phase diagram

N. P. Ong[a] and Yayu Wang [a] *

[a] Department of Physics, Princeton University, Princeton, N.J. 08544, U. S. A.

We review results obtained from vortex-Nernst experiments in cuprates. Evidence for a loss of phase coherence at the Meissner transition T_{c0} is derived from vortex-like excitations that persist to high temperature T. Below T_{c0}, the Nersnt signal provides a determination of the upper critical field H_{c2} vs. doping x. Implications for the cuprate phase diagram are discussed.

The vortex-Nernst effect is a highly sensitive probe for detecting vortex motion in a type II superconductor [1]. In the past 3 years, we have used it to map out the region in the field-temperature (H-T) plane in which vorticity may be observed [2,3,4,5]. The results provide a fresh perspective on the cuprate phase diagram which we sketch here. When a superconductor (in the vortex-liquid state) is exposed to a weak gradient $-\nabla T||\hat{\mathbf{x}}$ in a field $\mathbf{H}||\hat{\mathbf{z}}$, vortices diffuse down the gradient with velocity $\mathbf{v}||\hat{\mathbf{x}}$. As each vortex *core* crosses the line between a pair of transverse voltage electrodes, the 2π phase slip of the condensate phase leads to a Josephson E field given by $\mathbf{E} = \mathbf{B} \times \mathbf{v}$. The Nernst signal is defined as $e_y = E_y/|\nabla T|$. In cuprates, Nernst experiments were initially conducted on optimally-doped samples [6].

In extending the experiments to underdoped $La_{2-x}Sr_xCuO_4$ (LSCO), Xu *et al.* [2] observed that e_y persists to temperatures 50-100 K above T_{c0}. Figure 1 shows several curves of e_y in underdoped LSCO ($x = 0.12$). Below the zero-field transition temperature $T_{c0} \simeq 29$ K, $e_y(T, H)$ is initially zero until the melting field line $H_m(T)$ is exceeded (for e.g., at 5 T in the curve at 10 K).

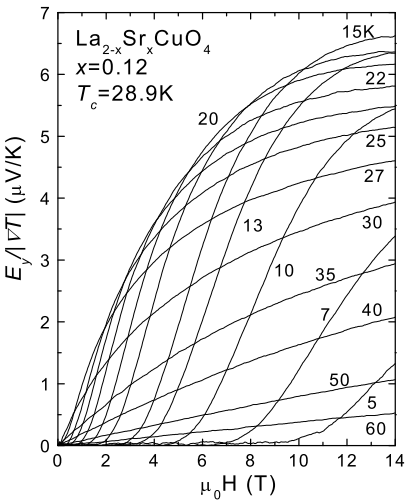

Figure 1. Field dependence of Nernst signal e_y in LSCO ($x = 0.12$) at T above and below T_{c0}. From Ref. [3].

In the liquid state, e_y climbs rapidly to attain a broad maximum near 14 T. As we warm to T_{c0}, we find that the maximum in e_y (curve at 30 K) is not much smaller than the low-T maxima. If e_y is linear in H in weak fields (above T_{c0}), we may define the Nernst coefficient as $\nu = e_y/B$ ($B \to 0$). Above T_{c0}, ν falls slowly and remains observable to ∼130 K [2,3,7].

*The research reported is a collaboration with Z. A. Xu, S. Uchida, S. Ono, Yoichi Ando, G. Gu, Y. Onose, Y. Tokura, D. A. Bonn, R. Liang, and W. N. Hardy. We acknowledge support from the U. S. National Science Foundation (NSF), the U. S. Office of Naval Research, and the New Energy and Industrial Technology Developmental Organization of Japan. Some of the experiments were performed at the National High Magnetic Field Lab. (NHMFL), a facility supported by NSF and the State of Florida.

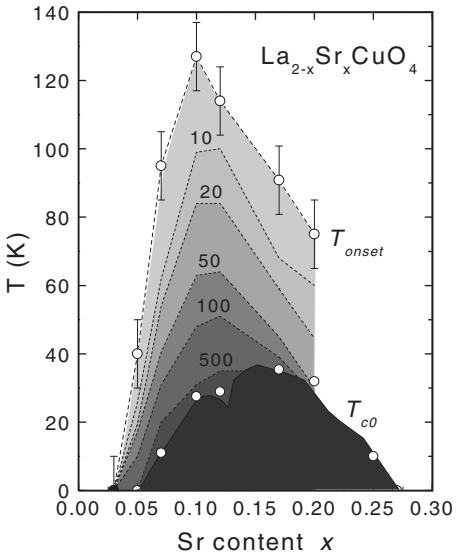

Figure 2. Phase diagram showing contours of the Nernst coefficient ν above the critical transition line T_{c0} vs. x in LSCO. The number at each contour line is the value of ν in nV/KT. Note that all contours and the onset line T_{onset} peak near $x = 0.10$. From Ref. [3].

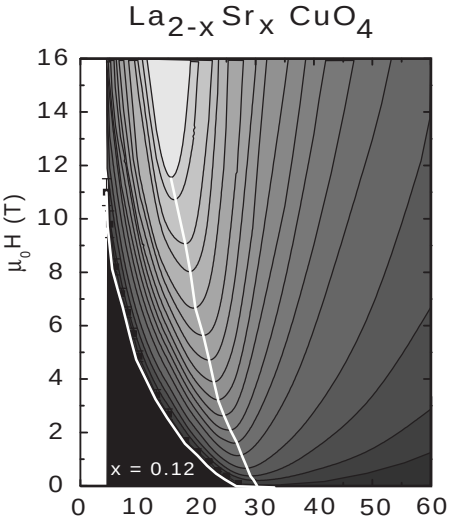

Figure 3. Contour plot of the Nernst signal $e_y(T, H)$ in the H-T plane for LSCO $x = 0.12$. Light grey indicates regions with largest value of e_y, while black indicates $e_y = 0$ (vortex solid). The melting field $H_m(T)$ (ridge field $H^*(T)$) is the lower (upper) white curve.

The findings of Xu *et al.* [2] imply that vortex-like excitations exist above T_{c0} high into the pseudogap state. What is the onset temperature T_{onset}? At high T, where the vortex-Nernst coefficient ν becomes comparable to that of the carriers, it is necessary to measure the hole thermopower and Hall angle to isolate the vortex signal [3]. The derived phase diagram for LSCO shows that T_{onset} lies high above T_{c0} (Fig. 2). A notable feature is the prominent maximum of T_{onset} and all the contours at $x \sim 0.1$ (instead of 0.17). These results provide strong evidence that, over a large part of the phase diagram, significant condensate strength exists above T_{c0}. This raises the possibility that the line T_{c0} vs. x measured by the Meissner effect actually corresponds to the loss of long-range phase coherence instead of the vanishing of the superconducting complex order parameter $\hat{\psi}(\mathbf{r})$ [8,9].

Below T_{c0}, the dependence of $e_y(T, H)$ on T and H changes in a characteristic way as a function of doping. An effective way to provide a broad overview is display $e_y(T, H)$ as a contour map in the H-T plane [4]. In Fig. 3 (for LSCO, $x = 0.12$), e_y attains its largest value in the light areas, while it is zero in the black areas (in the vortex-solid phase). As the melting line $H_m(T)$ line is crossed in a fixed-H scan, the signal rises steeply to a maximum before decreasing slowly on the high-T side. The locus of the maxima defines a 'ridge' field $H^*(T)$. We stress that, in the contour map, no crossover line or phase boundary separates the vortex liquid phase from a putative normal state above T_{c0}.

In low-T_c superconductors, e.g. $2H$-$NbSe_2$, the upper critical field line $H_{c2}(T)$ unambiguously separates the Abrikosov state from the normal state. Moreover, H_{c2} approaches zero linearly as

$H_{c2} \sim (T_{c0} - T)$. Where is H_{c2} in the cuprates? The received wisdom seems to be that (i) H_{c2} in cuprates is completely obliterated by strong fluctuations and not observable, or (ii) the 'real' H_{c2} line should be identified with $H_m(T)$ since this is the line at which superfluidity vanishes. Our experiments do not support either view.

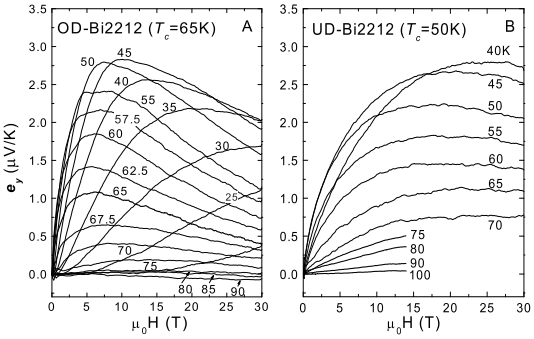

Figure 4. Curves of e_y vs. H in overdoped (Panel A) and underdoped (Balnel B) Bi 2212. The Nernst signal peaks at 5-10 T in the overdoped sample but at larger H (15-30 T) in the underdoped. Bold lines are curves taken at T_{c0} in both samples. From Ref. [5]

In our quest for H_{c2}, we have extended measurements to 30 T (later to 45 T) at NHMFL. The higher fields immediately revealed that, in every sample, the curve of e_y vs. H invariably has a 'tent' profile. To understand its significance, we examined how e_y behaves in thin-film PbIn. There, e_y (derived from the Ettingshausen effect [10]) increases rapidly when the vortex lattice is depinned, then rises to a sharp maximum before falling to zero linearly with the difference field $H_{c2} - H$ (Fig. 5c). The decrease reflects the field suppression of the condensate amplitude.

In the cuprates, the contour plots provide a road map for the field needed to get over the ridge

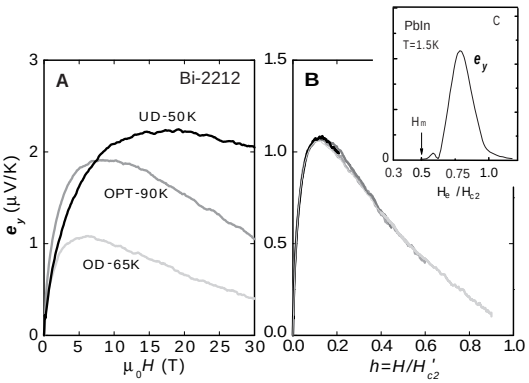

Figure 5. Panel A: Curves of e_y taken at T_{c0} in overdoped (OD), optimum-doped (OPT) and underdoped (UD) Bi 2212. Panel B shows the collapse of the 3 curves onto the template curve derived from $Bi_2Sr_{2-y}La_yCuO_6$ ($y = 0.4$) when plotted versus the reduced field $h = H/H_{c2}$. Panel C shows e_y vs. H in PbIn (from an Ettingshausen experiment [10]). Modified from Ref. [5]

field $H^*(T)$. Beyond $H^*(T)$, e_y falls monotonically. By extrapolating to the field at which it vanishes, we may determine H_{c2}. In overdoped cuprates, fields of ∼10 T are enough to go over the ridge. Figure 4A shows the tent profile of e_y in overdoped $Bi_2Sr_2CaCu_2O_{8+y}$ (Bi 2212) revealed in a field of 30 T. These curves extrapolate to zero near 50 T which we take to be the value of H_{c2} at this doping. The profile in $Bi_2Sr_{2-y}La_yCuO_6$ (Bi 2201) (Fig. 5B) is closely similar in shape. As H approaches 50 T, e_y decreases by a factor of 10 to approach zero at 48 T.

In underdoped hole-type cuprates, however, a field of 30 T is barely sufficient to get to the top. Figure 4B displays curves of e_y in underdoped Bi 2212. In comparison with Panel A, the curves in Panel B appear to be more stretched out along the field axis. From results on several cuprate families, we have found that this trend is ubiquitous. It takes a much larger field to reach the maximum in e_y in underdoped cuprates (Fig. 5A). To make the trend quantitative, we exploit a scaling property of e_y vs. H near T_{c0} that we

uncovered in Bi-based cuprates. By re-plotting the ratio $e_y(H)/e_{y,max}$ versus the reduced field H/H_{c2}, we can collapse curves from samples with different x onto a common curve (Fig. 5B). Moreover, the similarity applies to curves measured in Bi 2212, 2201 and 2223 (near their respective T_{c0}). The curve for Bi 2201 at 30 K (Fig. 5B) which extends to 45 T serves as the template against which curves from other Bi-based cuprates can be compared.

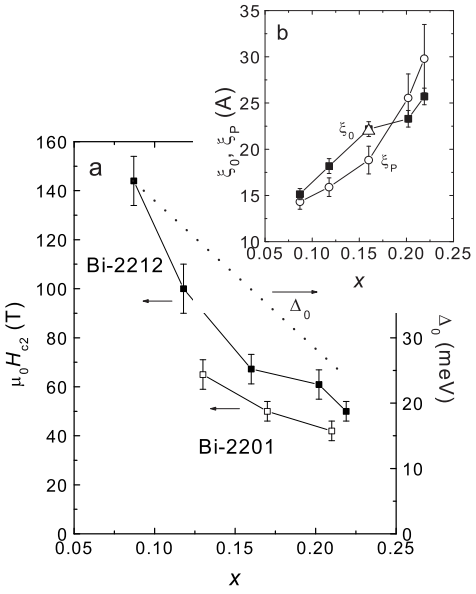

Figure 6. (Main panel) Variation of H_{c2} with x in Bi 2212 and Bi 2201. The dashed line is the ARPES gap amplitude Δ_0 in Bi 2212 [13]. The inset compares ξ from H_{c2} (solid squares), ξ_P from Δ_0 (open circles) and ξ from STM spectroscopy (open triangle). From Ref. [5].

Values of H_{c2} derived from the scaling technique are plotted in Fig. 6 for Bi 2201 and Bi 2212. The H_{c2} values confirm the qualitative trend inferred from Fig. 4. For Bi 2212, H_{c2} is ∼140 T at $x = 0.08$, and falls steeply as x increases to 0.25. The decrease in Bi 2201 is quite similar but the overall values are smaller. In LSCO, unfortunately, the large values of H_m make the scaling technique inapplicable. However, H_{c2} determined by a different method [4] shows a closely similar trend.

Using the equation $H_{c2} = \phi_0/2\pi\xi^2$, we have computed the coherence length ξ which is plotted in the inset to Fig. 6. At $x = 0.08$, ξ is small (1.5 nm), but it steadily increases to 3.0 nm at $x = 0.22$. Pan *et al.* [11] have measured the decay length of quasiparticle density of states near a vortex core in optimally doped Bi 2212 by STM and obtained 2.2 nm. This is in good agreement with our results (open triangle). ARPES measurements of the gap amplitude Δ_0 in Bi 2212 by Harris *et al.* [12] and Ding *et al.* [13] show that Δ_0 extends to T significantly higher than T_{c0} and decreases monotonically with increasing x. We may use the relation $\xi_P = \hbar v_F/\alpha\Delta_0$ to define the Pippard length ξ_P (where v_F is the Fermi velocity and α is a number). Converting the ARPES gap [13] to ξ_P, we find that it agrees with our coherence length if α is chosen to be $\frac{3}{2}$ (open circles in inset). This persuades us that the 3 experiments are measuring the same length scale in Bi 2212. Hence we should properly interpret Δ_0 as the superconducting gap amplitude. Its magnitude dictates the shortest length scale over which we may bend $\hat{\psi}(\mathbf{r})$, and matches rather well the vortex core size determined from STM and our H_{c2} measurements.

From Fig. 6, we infer that, as x increases from 0.08, the coherence length which measures the Cooper pair size expands monotonically. This immediately implies that the pairing strength starts out being very large in underdoped cuprates, but falls monotonically with increased doping. At $x = 0.08$, we have tightly bound pairs of size comparable to the interpair spacing. The sparse density forms a condensate with small superfluid density ρ_s. Although the onset temperature for pair formation is at high T (possibly higher than $T_{onset} \sim$ 130 K), the small ρ_s implies low phase stiffness. Long-range phase coherence appears at a T_{c0} that is very low. As we increase x towards optimal, ρ_s increases rapidly so that long-range phase co-

herence appears at a higher T_{c0}, but we pay the price of reducing the pairing strength. Finally, in the overdoped regime, the rapid decrease of the pairing strength forces T_{c0} to smaller values despite the large superfluid density available. The two conflicting trends appear to account naturally for the dome-shape T_{c0} curve that is universal in hole-doped cuprates. The end-point of $H_m(T)$, which is sensitive to ρ_s, determines T_{c0} (see below). However, the low-temperature onset of long-range phase coherence determined by ρ_s is emphatically distinct from the high energy scale of the pairing potential which induces pair formation above 130 K in the underdoped regime.

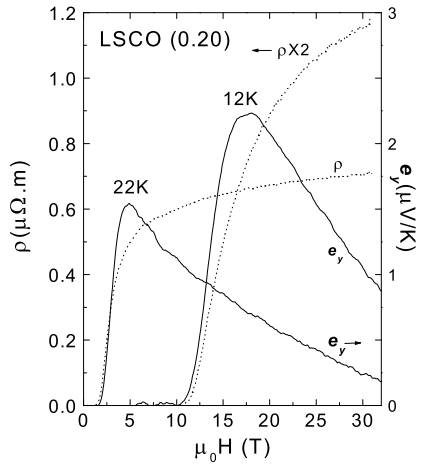

Figure 7. The flux-flow resistivity ρ and Nernst signal e_y vs. H at 22 K and 12 K in LSCO ($x = 0.20$).

Further clarification derives from a comparison of e_y with the flux-flow resistivity ρ (Fig. 7). As H exceeds H_m at 22 K, both e_y and ρ rise nearly vertically. The field-scale at which ρ forms a knee, often taken to define 'H_{c2}', is seen to be just slightly larger than $H^* \simeq 5$ T (where e_y peaks). However, it is quite apparent that the vortex signal remains substantial up to the much larger value of $H_{c2} \sim$45 T determined by $e_y \to 0$. The same discrepancy is apparent at 12 K. Flux-flow resistivity can be a rather misleading probe of the vortex state in cuprates.

Figure 7 illustrates the difference between the H dependence of ρ in the vortex liquid state in cuprates and Bardeen-Stephen behavior [1]. Instead of a linear increase from zero to the normal-state value $\rho_N(T)$ at H_{c2}, ρ rises steeply by a large fraction (~ 0.6) of ρ_N between H_m and H^*, and then gradually asymptotes to ρ_N. At $H > 2H^*$, the vortex liquid is indistinguishable from the 'normal state' using ρ alone. By contrast, the difference is apparent in e_y. In the strongly dissipative region above H_m (at low T), long-range phase coherence is absent because of the rapid mobility of the vortices. Nonetheless, *local* phase rigidity remains to support a high density of vortices. The Nernst signal detects the phase singularity at their cores and allows us to extrapolate to the field scale at which the vortices are finally suppressed.

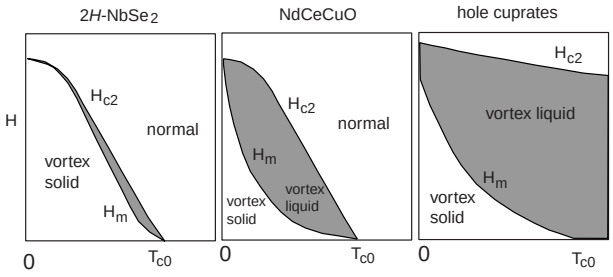

Figure 8. The fields H_m and H_{c2} in the H-T plane in $2H$-$NbSe_2$, $Nd_{2-x}Ce_xCuO_4$, and hole-doped cuprates. In the last (third panel), H_{c2} is nearly T independent below T_{c0}, and the vortex liquid extends well above T_{c0} .

The loss of phase coherence when H exceeds H_m at low T is closely similar to the loss of phase coherence when T is increased above T_{c0} in a weak H. In this light, the initial findings of Xu *et al.* [2] may be seen as the smooth continuation of the

low-T vortex-liquid state to the T axis above T_{c0}.

To place these results in perspective, we compare hole-doped cuprates with the electron-doped cuprate $Nd_{2-x}Ce_xCuO_4$ (NCCO). In the latter, the vortex-Nernst signal rapidly vanishes when T_{c0} is exceeded [5]. The H_{c2} line inferred [5] from e_y vs. H is just that expected from BCS theory. The absence of vortex excitations above T_{c0} in $Nd_{2-x}Ce_xCuO_4$ is likely related to the absence of a pseudogap state above T_{c0}. Figure 8 compares the H-T phase diagrams for $2H$-$NbSe_3$, $Nd_{2-x}Ce_xCuO_4$ and the hole-doped cuprates. The first two have a BCS-like phase diagram in which H_{c2} terminates at T_{c0}. The vortex state is clearly distinguished from the normal state (the vortex liquid state occupies a much larger area in NCCO). In hole-doped cuprates, H_{c2} falls slowly with T (if at all) and seems to approach zero at very high T. The vortex liquid state adiabatically continues to T above T_{c0}, and no phase boundary terminating at T_{c0} is observable.

This viewpoint emphasizes that, in hole-doped cuprates, the Meissner transition at T_{c0} is invariably the end-point T_m of the melting line. The zero-H transition occurs as soon as the population of thermally excited vortex-antivortex pairs are trapped in the vortex solid phase. While this picture differs from the BCS scenario, it is also distinct from what happens at a *strictly* 2D Kosterlitz-Thouless (KT) transition. In MoGe [14], for instance, T_m lies well below T_{KT}. Interestingly, as we go from $YBa_2Cu_3O_7$ to LSCO to Bi 2212 and Bi 2201 (increasing anisotropy), the T dependence of H_m flattens out to approach the 2D KT situation (but, at low enough H, H_m always ends at T_{c0}). The c-axis coupling plays a central role in establishing 3D long-range phase coherence.

Finally, we note that, along the classical axis T at $H = 0$, there is a large temperature interval between the mean-field transition scale (perhaps T^*) and the observed T_{c0}. If we scan along the 'quantum' axis H at $T = 0$, will we find that the melting field $H_m(0)$ lies significantly below H_{c2}? The nature of the state in between should be quite unusual.

REFERENCES

1. For a review, see Y. B. Kim and M. J. Stephens in *Superconductivity Vol. II*, ed. R. D. Parks (Dekker, NY, 1969).
2. Z. A. Xu *et al.*, Nature **406**, 486 (2000).
3. Yayu Wang *et al.*, Phys. Rev. B **64**, 224519 (2001).
4. Yayu Wang *et al.*, Phys. Rev. Lett. **88**, 257003 (2002).
5. Yayu Wang *et al.*, Science, **299**, 86 (2003).
6. S. J. Hagen *et al.*, Phys. Rev. B **42**, 6777 (1990); H. C. Ri *et al.*, Phys. Rev. B **50**, 3312 (1994); J. A. Clayhold *et al.*, Phys. Rev. B **50**, 4252 (1994).
7. C. Capan *et al.*, Phys. Rev. Lett. **88**, 056601 (2002).
8. V. J. Emery and S. A. Kivelson, Nature **374**, 434 (1995); G. Baskaran, Z. Zou and P. W. Anderson, Solid State Commun. **63**, 973 (1987).
9. J. Corson *et al.*, Nature **398**, 221 (1999).
10. Felix Vidal, Phys. Rev. B **8**, 1982 (1973).
11. S. H. Pan *et al.*, Phys. Rev. Lett. **85**, 1536 (2000).
12. J. M. Harris *et al.*, Phys. Rev. B **54** 15665 (1996); A. G. Loesser *et al.*, Science **273**, 325 (1996).
13. H. Ding *et al.*, Phys. Rev. Lett. **87**, 227001 (2001).
14. A. Yazdani *et al.*, Phys. Rev. B **50**, 16117 (1994).